Beyond 100 Gb/s: Capacity, Flexibility, and Network Optimization

Kim Roberts, Qunbi Zhuge, Inder Monga, Sebastien Gareau, and Charles Laperle

***Abstract*—In this paper, we discuss building blocks that enable the exploitation of optical capacities beyond 100 Gb/s. Optical networks will benefit from more flexibility and agility in their network elements, especially from coherent transceivers. To achieve capacities of 400 Gb/s and more, coherent transceivers will operate at higher symbol rates. This will be made possible with higher bandwidth components using new electro-optic technologies implemented with indium phosphide and silicon photonics. Digital signal processing will benefit from new algorithms. Multi-dimensional modulation, of which some formats are already in existence in current flexible coherent transceivers, will provide improved tolerance to noise and fiber nonlinearities. Constellation shaping will further improve these tolerances while allowing a finer granularity in the selection of capacity. Frequency-division multiplexing will also provide improved tolerance to the nonlinear characteristics of fibers. Algorithms with reduced computation complexity will allow the implementation, at speeds, of direct pre-compensation of nonlinear propagation effects. Advancement in forward error correction will shrink the performance gap with Shannon's limit. At the network control and management level, new tools are being developed to achieve a more efficient utilization of networks. This will also allow for network virtualization, orchestration, and management. Finally, FlexEthernet and FlexOTN will be put in place to allow network operators to optimize capacity in their optical transport networks without manual changes to the client hardware.**

***Index Terms*—Digital signal processing; Modulation formats; Optical coherent transceivers; Optical networks.**

I. Introduction

Network traffic has been increasing exponentially for the last few decades, and this trend is anticipated to continue for the next several years. This is driven by emerging high-bandwidth-demanding applications, such as cloud computing, 5G wireless, high-definition video streaming, and virtual reality [1]. To add to the high-capacity challenge, network services are becoming more dynamic and heterogeneous.

To illustrate the challenge, we look at a specific network, the Research and Education Network of ESnet. This network provides high-performance and high-capacity connectivity to all U.S. Department of Energy National Labs. Significant growth in scientific data, the number of data sets, and the evolution of scientific workflows has caused traffic to grow in excess of 70% a year. It is estimated that by 2025, this long-haul core network will have over 40% of its light paths carrying traffic in excess of 10 Tb/s and 10% with traffic in excess of 20 Tb/s. Therefore, to fulfill its mandate, ESnet must deploy state-of-the-art transmission technology that will enable the minimization of the transport cost and, if possible, allow the use of the installed capacity with the utmost flexibility. To satisfy these requirements, intensive research on optical communications has been conducted to reduce the cost per bit and increase the spectral efficiency of backbone networks [2].

Advanced coherent technologies in digital signal processing (DSP), modulation formats, and forward error correction (FEC) were commercially realized to exploit the capacity potential of fiber channels [3–5]. Very rapidly, the gap between the capacity of commercial systems and the Shannon limit was reduced to a few dBs or less, due to the deployment of high spectral efficiency formats and soft-decision FEC [6]. The architecture of coherent systems enables unprecedented flexibility for optical networks [7,8]. DSP allows for dynamic compensation of linear optical channel impairments, such as chromatic dispersion, leading to easy and fast rerouting of optical channels across disparate paths [9,10]. Modulation formats can be reconfigured to maximize the channel spectral efficiency for each specific link [11,12]. Bandwidths can be properly tuned according to capacity demand [8,13]. Functionalities are being developed within coherent receivers to monitor link conditions. Furthermore, sliceable coherent transceivers have been proposed, to accommodate heterogeneous traffic flows cost-effectively [8].

In legacy wavelength-division multiplexing systems, identical data rates are normally assigned to all channels, according to the worst-case end-of-life margin requirements. This results in a substantial excess margin, especially for the start of life of a network. In addition, the optical band is often sliced with a fixed 50 GHz grid. Those slices are narrowed by the optical filtering roll-off, resulting in two issues. First, the implementation of large-capacity, single-wavelength (>250 Gb/s) signals cannot be accommodated by these systems at regional or long-haul reaches since the optical bandwidth is larger than what is available (approximately 40 GHz passband) for the resulting light paths. The main reason is that for long reaches, a high

Manuscript received October 18, 2016; revised December 27, 2016; accepted January 10, 2017; published February 7, 2017 (Doc. ID 278885).

K. Roberts (e-mail: kroberts@ciena.com), Q. Zhuge, S. Gareau, and C. Laperle are with Ciena Corporation, Ottawa, Ontario K2H 8E9, Canada.

I. Monga is with Energy Sciences Network (ESnet), Berkeley, California 94720, USA.

https://doi.org/10.1364/JOCN.9.000C12

 Journal © 2017 Optical Society of America

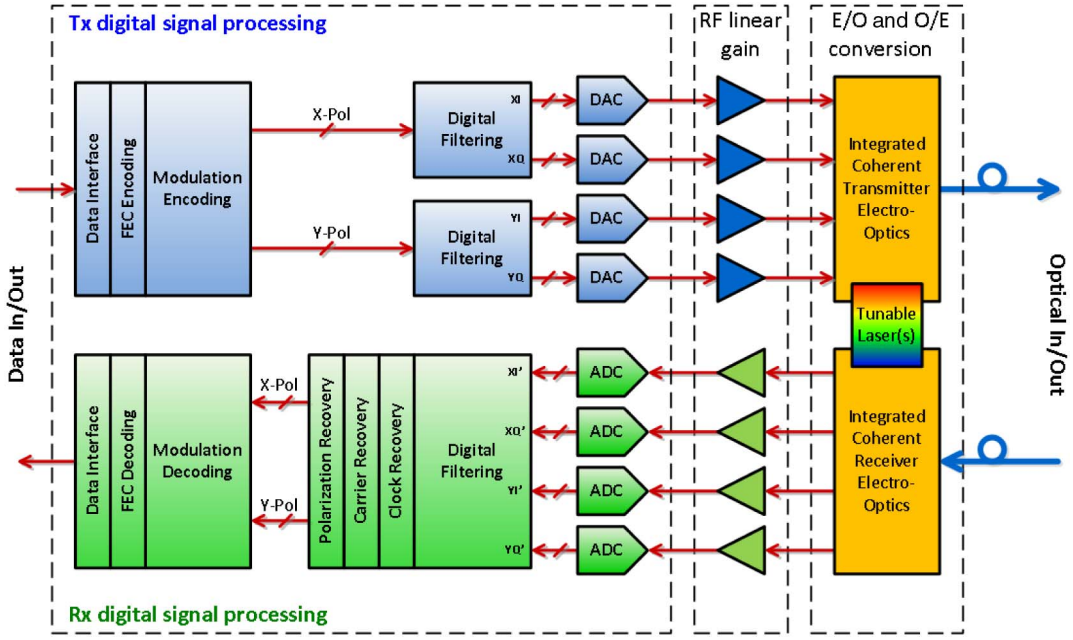

Fig. 1. Block diagram of a typical optical coherent transceiver.

bit rate would require a less complex constellation (for better noise tolerance) with a higher baud rate, which in turn means a large optical spectrum occupancy. However, for metro and data center interconnect (DCI) applications, there are solutions currently available up to 400 Gb/s on a single wavelength. Second, the bandwidth utilization is inefficient for the lower speed channels that do fit. A flexible grid, with 12.5 GHz bandwidth granularity and 6.25 GHz central frequency resolution [14], solves the above issues and enables heterogeneous traffic flows with uneven channel spacing. The flexibilities of a coherent transceiver can be leveraged to convert extra margins into capacity in order to maximize network efficiency.

This paper will discuss advanced hardware technologies based on indium phosphide (InP) and silicon photonics (SiP) for higher-bandwidth and lower-power components. Advanced digital approaches will also be presented. These will enable the successful realization of the next generation in coherent transceivers for channel capacities of 400 Gb/s and beyond to provide better performance in flexible networks.

The paper is organized as follows: in Section II, we discuss coherent systems, which are crucial for next-generation optical networks. In Section III, we look at the requirements and prospects for the next step in the evolution of coherent technology. High-bandwidth components are discussed in Section IV. These form the basic building blocks for coherent modems carrying 400 Gb/s and beyond. In Section V, we review enabling technologies, such as advanced modulation formats, nonlinear digital compensation, frequency-division multiplexing, and FEC. The harvesting of margin currently available in a network is presented in Section VI, along with network virtualization, orchestration, and management software. FlexEthernet and FlexOTN are presented in Section VII.

II. Commercial Realities

Currently deployed commercial coherent transceivers typically transmit 50 to 200 Gb/s per wavelength within a fixed 50-GHz grid spacing. Applications span metro, regional, long-haul, and submarine distances [4]. In the case of metro and DCI applications, higher capacities, such as 250 and 400 Gb/s, are also available for the same grid spacing.

Figure 1 shows the block diagram of a typical optical coherent transceiver. Figure 2 shows a Ciena WaveLogic 3 coherent transceiver and its DSP ASIC. This modem operates at 35 Gbaud and delivers capacities from 50 to 200 Gb/s in steps of 50 Gb/s. This modem is utilized in all applications from metro at 200 Gb/s to trans-Pacific submarine applications at 50 Gb/s. The optical bandwidth of the modulated signal is about 38 GHz, making it compatible with a 50-GHz fixed grid or a flexible grid with a channel spacing as small as 37.5 GHz.

Fig. 2. Ciena WaveLogic 3 coherent transceiver and DSP ASIC with 50, 100, 150, and 200 Gb/s capability.

III. Commercial Prospects

More innovations in optical transceiver technology are desired to further reduce the cost per bit and increase network efficiency. The commercial requirements of next-generation coherent transceivers will be to enable higher capacity, more flexibility, and lower power consumption per bit.

A. 400 Gb/s and Beyond

A 400 Gb/s transmission on a single wavelength offers the opportunity for a lower cost per bit. To generate a 400 Gb/s signal, both the symbol rate and modulation format cardinality need to be increased relative to current 100 Gb/s QPSK modems. For example, 56 Gbaud 16-QAM and 43 Gbaud 64-QAM using a commercial dual-polarization InP modulator have been demonstrated [15]. An important challenge in implementing the 16-QAM solution is to have all the optoelectronic components operating at a high symbol rate [16]. The major challenge of implementing the 64-QAM solution is the lower total noise tolerance, relative to the transceiver implementation noise, which severely noise limits the transmission distance. Each of these approaches has challenges that will impact the overall system performance. Other tradeoffs between increasing the symbol rate and/or using more complex constellations may yield different results. For example, the use of a lower-order modulation format, such as 32-QAM, with a moderate increase in the symbol rate will extend the transmission distance.

It is anticipated that 400 Gb/s per wavelength systems will first be deployed in moderate-distance metro and DCI applications. Mitigation of the analog transceiver noise and distortion is going to be crucial for achieving the required performance cost-effectively, as will be discussed in detail in Section IV.

B. More Capacity

Several methods are available to increase the overall capacity of a system. The most obvious one is to widen the amplified spectrum. For example, adding an L-band over a C-band system [17,18] more than doubles the overall capacity at a constant spectral efficiency (the C-band is 35 nm wide, and the L-band is 60 nm wide). In this paper, the focus is on solutions originating in the modem.

Most currently deployed commercial systems deliver a spectral efficiency of about 1 to 5 bit/s/Hz, depending upon the noise and nonlinearity accumulated while traversing the desired distance. The paths to improve the spectral efficiency are threefold: first, the transceiver internal noise, caused by quantization noise, RF driver nonlinearity, bandwidth limitation, Tx and Rx I/Q errors, clock jitter, and DSP impairments, needs to be reduced. This is especially important in short-distance transmissions, where the link accumulated noise and distortion are relatively small with respect to the internal noises. Second, advanced modulation formats with higher noise tolerance and stronger FEC, with a higher coding gain, need to be developed. Third, fiber nonlinearity mitigation and compensation techniques can be used to reduce the fiber nonlinear noise. Technologies to achieve this will be discussed in Section V.

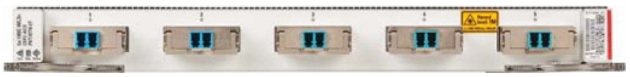

Fig. 3. Interface card with five CFP2-ACO pluggable transceivers.

C. Smaller Capacity Granularity

In addition to higher capacity per wavelength and longer optical reaches, finer granularity in data rates also lowers the cost per bit. This cost-effectiveness improvement occurs by enabling a more complete exploitation of the signal-to-noise ratios (SNRs) available in diverse and dynamic optical networks [11,12]. For instance, a 16% capacity gain has been observed in a Microsoft cloud network by reducing the granularity from 50 to 25 Gb/s [19]. New standards like FlexEthernet and FlexOTN, to be discussed in Section VII, provide a 25 Gb/s service level granularity to take advantage of new modulation methods.

D. Port Density

The density of DWDM optical interfaces in a high-capacity switch is important to optimize the switch fabric and switch infrastructure cost-effectiveness. This provides motivation for the use of multiple modems per interface card. When the optical transducers attract a significant proportion of the cost and failure rate of a card, it is useful to have those transducers within hot-swappable plugs. Figure 3 shows how up to five coherent metro modems can fit onto one interface card, with five CFP2-ACO plugs. To implement the modem into compact, field-replaceable plugs, electro-optic components based on InP and SiP, with their high-bandwidth and high baud rate capabilities, will play an important role. These are discussed in the next section.

IV. High-Bandwidth Components

The main drivers for the demand of new optical components are smaller size, lower power consumption, and higher bandwidth. High-bandwidth (>40 GHz) optical components are key enablers for capacities of 400 Gb/s and beyond.

A. Electrical Components

High-bandwidth electrical components in the transceiver include digital-to-analog converters (DACs), variable gain amplifiers (VGAs), drivers on the transmitter

side, transimpedance amplifiers (TIAs), analog-to-digital converters (ADCs), and VGAs on the receiver side. TIAs can also have adjustable gain.

DACs at the transmitter allow the use of DSP for equalization, and the capability of a wealth of software-definable modulation formats from a single transceiver. ADCs at the receiver precede equalization, clock, carrier, polarization recovery, and modulation decoding by the DSP. Six-bit DACs and ADCs are sufficient for modulation formats up to 16-QAM. However, higher modulation formats (32-QAM and above) require higher SNRs, which dictate a minimum converter resolution of 8 bits. The important design parameters of high-speed DACs and ADCs include [3] bit resolution, sample rate, signal-to-noise-plus-distortion ratio, clock speed, jitter, and power dissipation. A 100 GSa/s 6-bit DAC has been realized in BiCMOS technology to demonstrate 400 Gb/s transmission, with a dual-channel 32 Gbaud dual-polarization 16-QAM signal [20]. An 8-bit ADC has been demonstrated up to 90 GSa/s [21]. Figures 4 and 5 show the measured ENOB of 68 GSa/s 8-bit DAC and ADC in 28-nm CMOS silicon-on-insulator (SOI) technology. These DACs and ADCs are suitable for next-generation 400 Gb/s optical coherent transceivers.

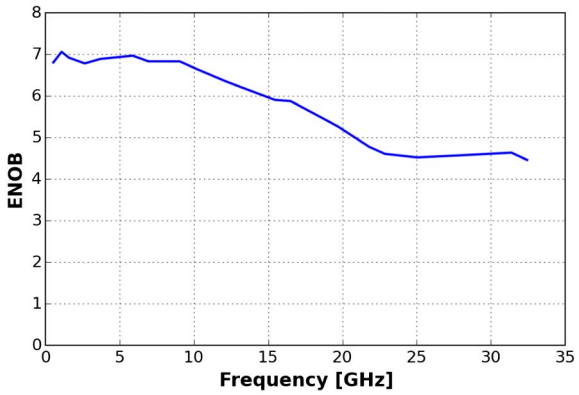

Fig. 4. Measured ENOB of a 68 GSa/s 8-bit DAC in 28-nm CMOS SOI technology.

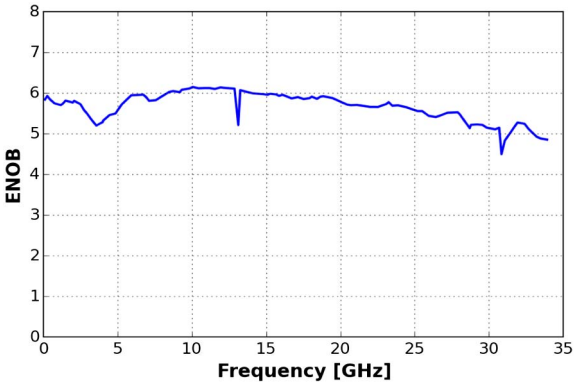

Fig. 5. Measured ENOB of a 68 GSa/s 8-bit ADC in 28-nm CMOS SOI technology.

VGAs are used in both the transmitter and receiver. In the transmitter, they adjust the amplitude and equalization of each tributary signal going to the driver and modulator so the four tributaries have the same amplitude (I/Q balance). In the receiver, the VGAs adjust the amplitudes of the signals going to the ADCs to maximize the input level to each ADC. The result is the best SNR while not overdriving the ADCs' input.

Drivers are an essential part of the transmitter. They amplify the modulating signals to drive the optical modulator, maximize the optical power at the output of the transmitter, and maximize the optical SNR.

Linearity of the electrical components is necessary to generate and receive the electrical and optical fields as faithfully as possible. Combined with the large bandwidth required for high baud rates, this makes the design of these components challenging. This is especially true for drivers that need to provide large voltage swings to the optical modulator (which usually also means a larger power dissipation).

Figures 6–8 show the measured frequency response of amplifiers with a >40 GHz bandwidth suitable for transmission at >70 Gbaud. Figure 6 shows the measured frequency response of a linear driver. It has a gain of 18 dB and can provide an output level of 5 $V_{peak\text{-}to\text{-}peak}$. Figure 7 shows the measured frequency response and chip layout of a VGA (a gain of 10 dB is shown). Its gain can be varied from 6 to 18 dB, its output level can be up to 1.5 $V_{peak\text{-}to\text{-}peak}$, and its output return loss is >10 dB up to 40 GHz. Figure 8 shows the measured frequency response and chip layout of a TIA for use in a coherent receiver module. Its transimpedance gain can be adjusted from 200 Ω to 4 kΩ, its input referred noise is 19 pA/$\sqrt{\text{Hz}}$, and its output return loss is >15 dB up to 40 GHz.

B. Electro-optical Components

There are two main high-bandwidth electro-optical components in the transceiver: a modulator in the transmitter, and an integrated coherent receiver in the receiver section. The components can be typically implemented in three

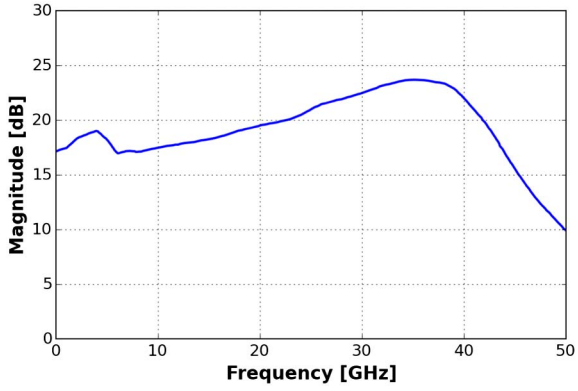

Fig. 6. Measured frequency response of wideband RF linear driver.

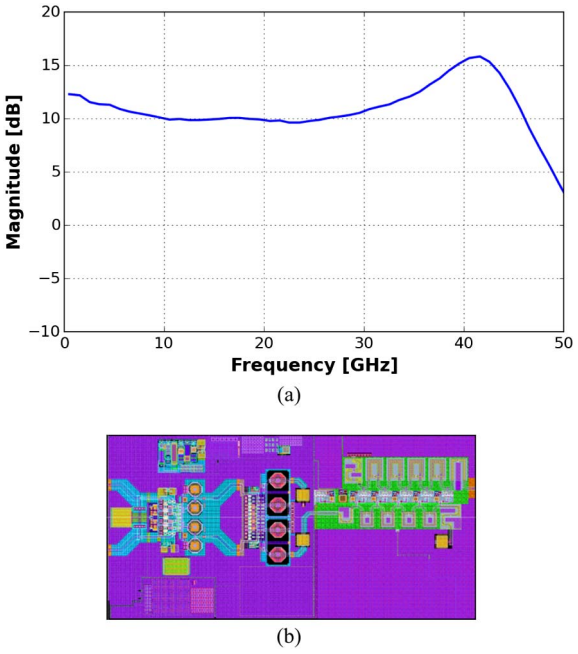

Fig. 7. VGA: (a) measured frequency response (10 dB gain shown) and (b) chip layout.

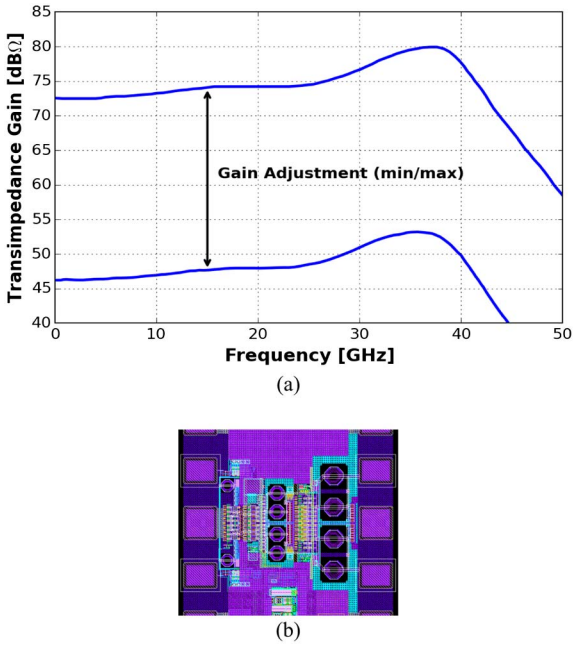

Fig. 8. TIA: (a) measured frequency response and (b) chip layout.

available technologies: lithium niobate ($LiNbO_3$), InP, and SiP. Each technology has its pros and cons; the choice of technology will depend on the application.

$LiNbO_3$ optical modulators have been used since early generations of intensity-modulation direct-detection transceivers at 2.5 Gb/s. The current technology integrates four Mach–Zehnder modulators in a superstructure, providing I/Q modulation on two orthogonal polarizations (dual-polarization I/Q modulators) for coherent transceivers. However, the main challenge with $LiNbO_3$ dual-polarization I/Q modulators is to obtain a high electrical bandwidth with a sufficiently low V_π in a compact package. While it is available for standard modem implementation, it does pose a specific challenge if the implementation of $LiNbO_3$ I/Q modulators needs to be done in a compact module/plug with limited heat dissipation capability.

InP is a semiconductor material and offers several advantages over the current $LiNbO_3$ technology. It has a small size (Fig. 9) and requires a low drive voltage, currently of the order of 1.5 V (V_π). This brings a significant power consumption reduction compared to $LiNbO_3$ modulators (less output swing required from the RF drivers). The potential to bring V_π below 1 V could eventually lead to designs where the drivers would be integrated in the DSP ASIC. The measured small-signal response of this modulator is shown in Fig. 10 with a 3-dB bandwidth of approximately 35 GHz. This type of module has been tested in a system, demonstrating very impressive results at 56 Gbaud (16-QAM) and 43 Gbaud (64-QAM) [15]. Bandwidths in excess of 50 GHz have also been demonstrated [22]. InP enables the integration of small form factor transponders for next generation linecards. Figure 11 shows an example of a small form factor modulator subassembly with dimensions of 30 mm × 14 mm.

SiP modulators with 40 GHz bandwidth have been demonstrated (Fig. 12, see also [23]). Efforts are currently underway for devices to work at 1.5 μm. Advanced packaging for SiP, through the use of ball-grid arrays, will enable

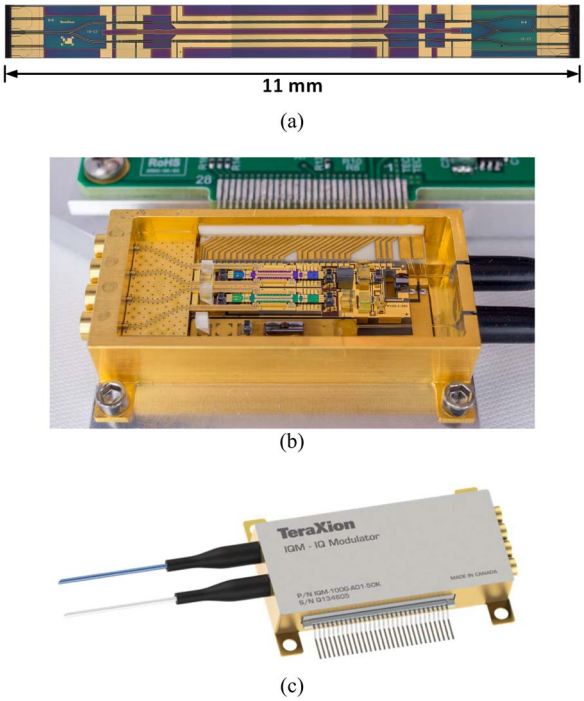

Fig. 9. InP modulator: (a) InP chip, (b) open, and (c) closed package for InP dual-polarization I/Q modulator, respectively.

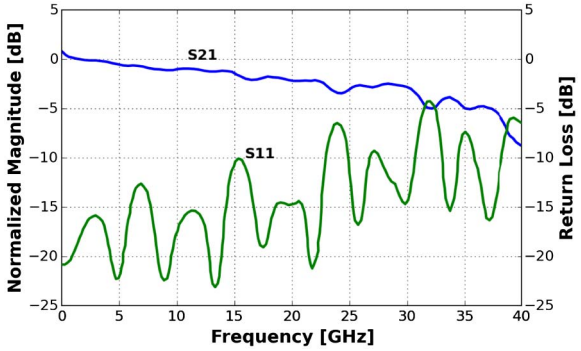

Fig. 10. Measured small-signal response (magnitude, S21 and return loss, S11) of the InP modulator inside the package shown in Fig. 9.

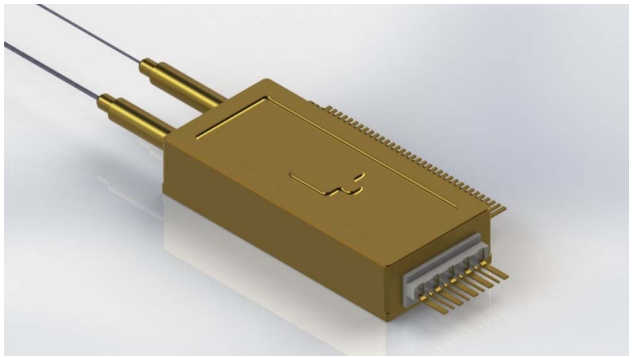

Fig. 11. InP small form factor modulator optical subassembly. Package dimensions: 30 mm × 14 mm.

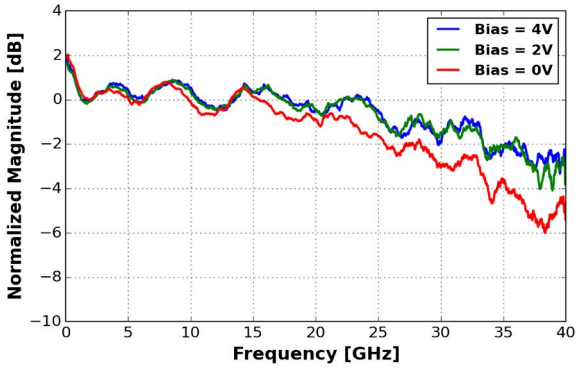

Fig. 12. Measured magnitude responses of a 40-GHz SiP modulator for different bias voltages. Magnitude is normalized at 1.5 GHz.

several advantages: further size reduction (smaller I/O ports), higher integration (higher I/O port count), uncooled, nonhermetic packaging, and proximity between optics and electronics. Figure 13 shows a small form factor SiP integrated coherent receiver module compared to an Optical-Internetworking-Forum-compliant version [24].

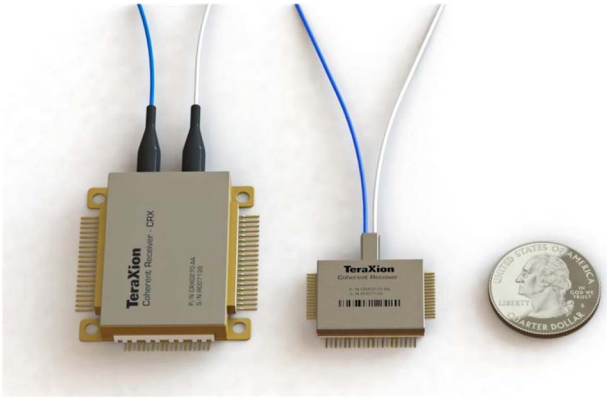

Fig. 13. SiP integrated coherent receiver modules.

The footprint of the small module is 23 mm × 18 mm. SiP could bring significant benefits, but innovative optical packaging technology is required, with closer proximity between the electronics and optics. Both InP and SiP will likely coexist for line-side applications.

V. Enabling Digital Technologies

In this section, advanced technologies in signal modulation, DSP, and FEC are introduced that enable unprecedented flexibilities and performance for optical communications.

A. Advanced Modulation Formats

Two-dimensional modulation formats have been used in the early generations of coherent systems for their implementation simplicity. Since then, the application space of coherent systems widened and higher tolerance to noise was required. To this effect, multi-dimensional modulation formats have been proposed [25–27], since they have the potential of achieving the needed higher noise tolerance, smaller data rate granularity, and mitigation of fiber nonlinearities. Figure 14 shows simulated constellations of two commercially implemented modulation formats: 8D-2QAM and 4D-8QAM. The baud rate of these signals is 35 Gbaud,

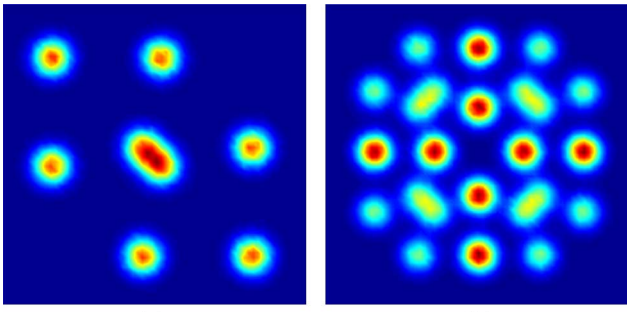

Fig. 14. Simulated constellations of multi-dimensional modulation formats: (a) 8D-2QAM and (b) 4D-8QAM.

and the root-raised-cosine filter roll-off factor is 0.14. The 8D-2QAM format has the same spectral efficiency as conventional BPSK, but an improved linear noise tolerance. This is achieved by increasing the minimum Euclidean distance and reducing the nonlinear interference by balancing the signal power and polarization [28]. As a demonstration of the significant improvements provided by these modulation formats, they have been deployed for trans-Pacific submarine links. The 4D-8QAM has the same spectral efficiency as conventional 8QAM. However, both the linear and nonlinear performances have been improved by manipulating the constellation in four dimensions.

Constellation shaping offers an ultimate gain of 1.53 dB for very high spectral efficiencies in an additive white Gaussian noise channel [29]. Both geometric and probabilistic shaping schemes have been demonstrated in optical communications to close the gap with the Shannon limit [30,31]. Probabilistic shaping assigns different probabilities to different constellation points when mapping from bits to symbols. In particular, higher probabilities are given to the constellation points with lower powers, leading to a reduced average power with the same Euclidean distance. In other words, the Euclidean distance is increased, resulting in a higher noise tolerance for the same transmitted power. As an additional benefit, probabilistic shaping also offers a means to tune the bits per symbol, and hence the capacity, with a very small granularity. Figures 15 and 16 show examples of simulated constellation shaping applied to 64-QAM and 128-QAM modulation formats. In both cases, the baud rate is 70 Gbaud.

Using these advanced modulation formats, one can expect that modems will be able to tailor quasi-continuously the in-fiber capacity. This, in turn, will allow researchers to design links with minimal extra margins over those required to ensure the performance until the end of the life of the system. This will allow researchers to improve the cost effectiveness of each light path by maximizing the delivered traffic while minimizing the need for electronic regeneration.

Figure 17 shows the delivered data rates of three different generations of Ciena WaveLogic (WL) modems, namely,

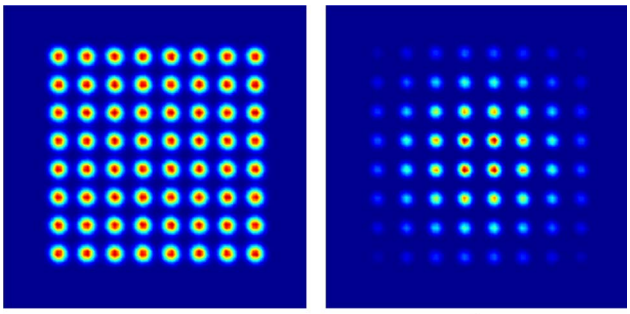

Fig. 15. Example of simulated constellation shaping for 64-QAM modulation format. (a) Without constellation shaping. (b) With constellation shaping.

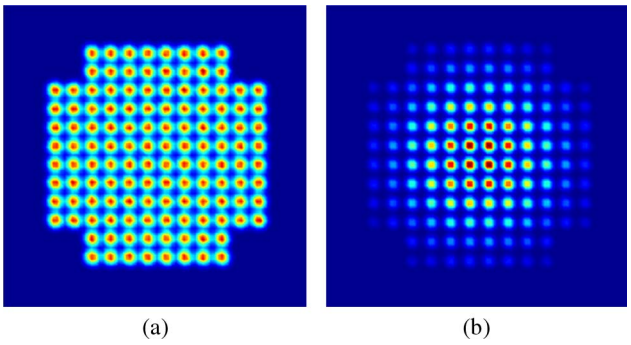

Fig. 16. Example of simulated constellation shaping for 128-QAM modulation format. (a) Without constellation shaping. (b) With constellation shaping.

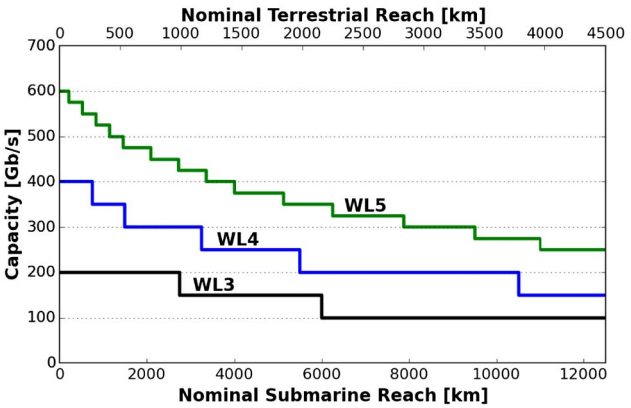

Fig. 17. Capacity versus reach for modems in Ciena's WaveLogic family. WL3 and WL4 have a granularity of 50 Gb/s, while WL5 has a granularity of 25 Gb/s. All three modems can serve applications ranging from metro to submarine.

the current WL3, and the new fourth and fifth generations,[1] WL4 and WL5, respectively. These cover distances up to 13,000 km for metro, regional, long-haul, and submarine applications. Specifically, WL3 and WL4 deliver rates with a granularity of 50 Gb/s. For WL5, probabilistic constellation shaping is employed to realize a granularity of 25 Gb/s. It can be seen that the data rate at the same distance is significantly increased for WL5 compared to WL3 and WL4. WL5 can achieve a maximum capacity of 600 Gb/s for metro and DCI applications. Note that the distances for terrestrial reaches are for "nominal" systems using a standard single-mode fiber with a uniform 21 dB of loss per 80 km and line amplifiers with a noise figure of 5 dB. The submarine applications use a low-loss large-effective-area fiber with a uniform 9.4 dB loss per 60 km and a line amplifier with a noise figure of 4.3 dB. Both systems include commercial margins for optical quality of service, which in general can range from a few dBs to several dBs and depend on the applications and hardware design.

[1]The new generations in the WaveLogic family, described as WL4 and WL5, are also called "WaveLogic Ai."

B. Nonlinear Digital Compensation

Digital nonlinear fiber compensation was first demonstrated in [32]. Two well-known algorithms are 1) digital backpropagation [33] and 2) perturbation nonlinear compensation [34]. Digital backpropagation is derived from the classical split-step Fourier method (SSFM). It requires FFT and IFFT operations to transform the signal between the time and frequency domains for nonlinear phase-noise compensation and dispersion compensation, respectively. Substantial efforts have been devoted to reduce the number of compensation stages (pairs of FFT and IFFT blocks) by better modeling the nonlinear effect with a larger dispersion in each stage [35]. Perturbation nonlinear compensation is derived from a closed-form solution of the nonlinear Schrödinger equation, obtained with the perturbation assumption. In this case, the nonlinear noise is considered as an additive noise. It is a summation of various combinations of data symbol triplets (product of three symbols) weighted by coefficients associated with link parameters. For a typical dispersion-unmanaged link, thousands of triplets are required in the nonlinear noise calculation. Reduction of the triplet number and the simplification of the triplet calculation have been active research topics to reduce the complexity of this technique [36,37]. Figure 18 shows an example of perturbation nonlinear compensation at the transmitter. The simulations are based on the experimental parameters described in [37] for propagation on a TrueWave Classic (TWC) fiber: one 35 Gbaud channel with the modulation format DP-16QAM and a root-raised-cosine filter with a roll-off factor of 0.14 is propagated across 10 spans of TWC fiber (80 km/span). The launch power is +2 dBm.

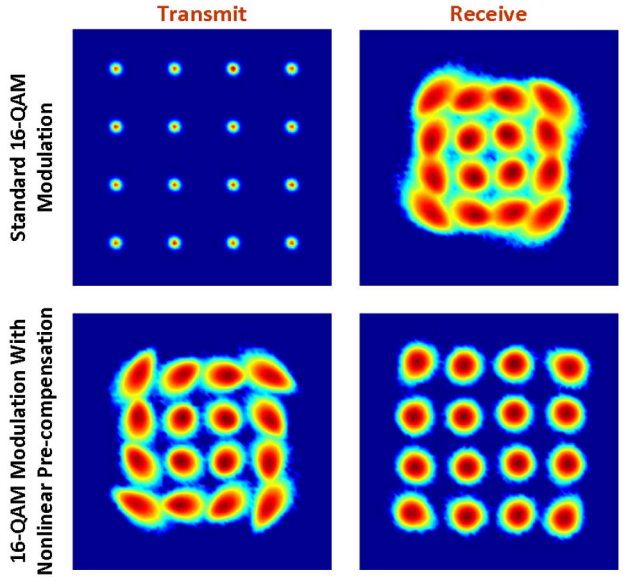

Fig. 18. Example of constellation with nonlinear pre-compensation. The simulations are based on the experimental parameters of [37] for propagation on TWC fiber.

Nonlinear compensation schemes normally require the information of the transmitted signals. Therefore, inter-channel digital nonlinear compensation is generally infeasible. Due to the limited amount of intra-channel nonlinearity in a DWDM system, a roughly 0.5 to 1 dB improvement in the Q-factor is achievable, depending on the system conditions. The improvement is expected to be smaller in a commercial implementation because of the power dissipation constraint in the circuit design. However, as the channel bandwidth increases through the increase of the symbol rate and the utilization of media channel configurations (which contain multiple network media channels, also called superchannels [38]), the intra-channel nonlinearity will become a larger portion of the nonlinear distortion experienced by future modems, and so the benefits of digital nonlinear compensation are anticipated to increase. According to the analysis in [39], the additional gain can be relatively large when we move from 100 to 400 Gb/s and 1 Tb/s systems, but after that, it starts to diminish.

C. Frequency-Division Multiplexing

Single-carrier signals were originally considered to have a higher nonlinear tolerance than multi-carrier signals because of the smaller power variance. However, it has been shown that frequency-division multiplexed signals with the appropriate number of subcarriers can improve the nonlinear tolerance for single-carrier signals in both simulations [40] and experiments [41]. The specific improvement will vary for different systems. For example, 15% and 9% increases in distance have been predicted using the enhanced Gaussian noise model and verified by SSFM simulations for 32 Gbaud QPSK and 16QAM SMF C-band systems, respectively [42]. A close improvement was demonstrated in a recent WDM transmission experiment [43]. Figure 19 shows the simulated spectra of frequency-division multiplexed signals with 1, 2, 4, and 8 subcarriers, each totaling 70 GBaud. Quasi-Nyquist pulse shaping is applied to each subcarrier to avoid inter-carrier interference.

The superchannel configuration with independent subchannels modulated using multiple lasers or a comb source is equivalently an optical FDM system. Hence, the nonlinear gain is inherently present compared with a comparable bandwidth single-carrier system. Digital FDM can also be applied to each subchannel in superchannel systems in order to achieve the ultimate gain of the symbol rate optimization.

D. Forward Error Correction

FEC attempts to correct all the errors caused by incorrect symbol decisions in the receiver due to both noise and nonlinearity [44]. Current commercial FECs for coherent optical transceivers are normally based on soft decision and use approximately 20% overheads. To achieve a further increase of the coding gain for next-generation coherent systems, more advanced FECs with overheads larger

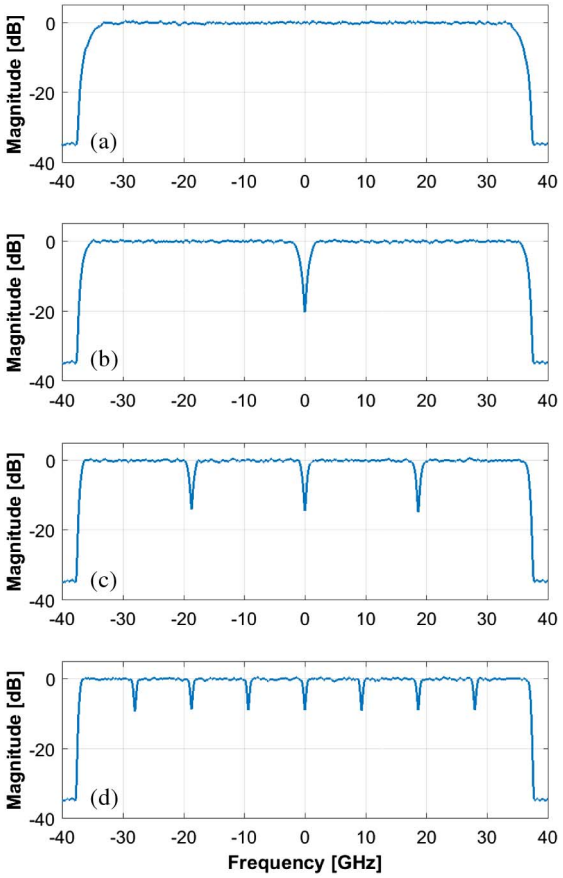

Fig. 19. Simulated spectrum segmentation for a 70 Gbaud signal with 1, 2, 4, and 8 subcarriers [(a)–(d), respectively].

than 25% are being developed [5]. Other design considerations include power consumption, latency, error floor, programmability, and so forth.

Before committing a design to silicon, the FEC design must be shown to be free of floor or flare [6] in the post-FEC bit error rate versus SNR curve. Since network operators often expect effectively zero loss of frame, the resource allocation and parameters of the soft-FEC decoding engine need to be tuned at the extreme limit of zero post-FEC errors. However, the software simulating a sophisticated FEC engine runs about eight orders of magnitude slower than a silicon ASIC. This poses a challenge in the simulation of low-probability events occurring when looking for the presence of an error floor or flaring.

To deal with this problem, powerful computing resources can be exploited. Recently, ESnet proposed leveraging the U.S. DOE expertise to accelerate the availability of high-capacity optical networking systems that could be deployed in their network. The application of DOE high-performance computing resources to the analysis of soft FEC design has been a very successful example of cooperation to benefit scientific progress.

Figure 20 shows the error correction performance of three generations of FECs. As a reference, the green curve (uncoded) is the bit error rate that is obtained when no FEC

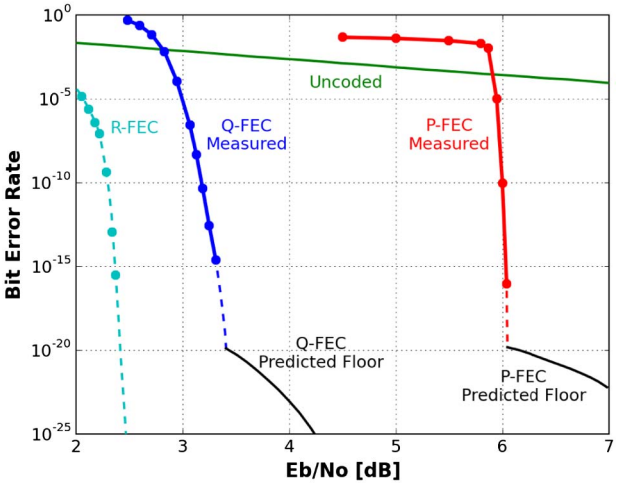

Fig. 20. Performance of various generations of FECs.

is used. P-FEC is a proprietary hard-decision FEC that was used in Ciena's WaveLogic 1 and WaveLogic 2 products and was implemented as a standalone FEC ASIC. Q-FEC uses soft decoding to achieve a 2.5 dB improvement in noise tolerance over the hard-decoded P-FEC. Q-FEC is used in WaveLogic 3 to correct signals to better than 1×10^{-15} with up to 3.4% input errors. This results in a net system margin gain of 11.5 dB with QPSK modulation and 12.7 dB with 16-QAM modulation. Q-FEC is implemented in Ciena's WaveLogic 3 DSP ASIC. Further improvement to the FEC algorithm will be designed in the R-FEC to enable up to a 1 dB additional margin over the Q-FEC.

As the R-FEC ASIC hardware does not yet exist, software simulations are used to validate the performance of the design. Eight million CPU hours of semi-analytic simulations on the Natural Environment Research Council High Performance Computer in Berkeley, California, have produced statistical confidence in the R-FEC results shown in Fig. 20. This has enabled the fine-tuning of the R-FEC CMOS circuit design. The approximately 1 dB performance improvement in the R-FEC will be exploited by network operators to obtain better spectral efficiency and/or reach. With all the technology advancements described in this section, it is expected that future generations of coherent transponders could achieve 1 Tb/s on a single carrier.

VI. Optical System Agility

Optical system agility based on high-capacity and flexible-rate transceivers can significantly increase the capacity of optical networks. As compared to a static network, provisioning the highest data rate according to the end-of-life margin of each link can enable significant gain in the overall network cost effectiveness [45,46]. As the network traffic becomes more dynamic and unpredictable, one-time planning may not yield spectrally efficient solutions. One example of how to accommodate this scenario and further increase the network capacity is the optical system agility architecture described in [47]. As illustrated in Fig. 21, the agility can be employed to transform the available extra

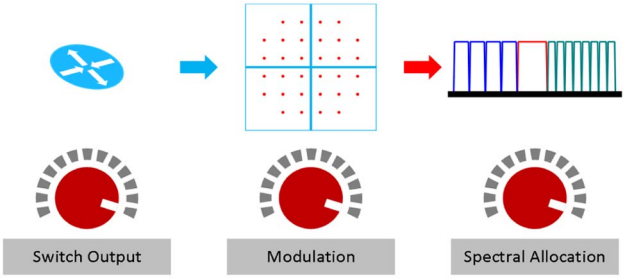

Fig. 21. Illustration of optical system agility.

margin into capacity. This concept uses the flexibility of coherent transceivers and photonics, coupled with software intelligence, to determine when and where it is appropriate to switch modulations or paths.

The utility of optical agility is well described in the following scenario. Upon initial deployment, when few wavelengths are used, the system has a higher system margin, due to less nonlinear noise, no aging, and so forth. At this early stage, higher spectral efficiency formats can be used to increase capacity. Since the first-in costs for the network are often critical, significant economic benefits can be achieved by deferring the purchase of additional coherent transponders. Other benefits of using optical agility include 1) simpler forecasting and reduced sparing costs, 2) faster response to on-demand service requests, and 3) CAPEX reduction for temporary high-bandwidth requirements.

The implementation of the optical agility requires both hardware and software elements. Using constellation shaping, the next-generation transceivers will deliver a capacity granularity of 25 Gb/s in the data rate, as discussed in the previous section. In addition, mapping between a flexible number of client signals and a variable line capacity is required. An efficient architecture can be realized based on centralized OTN or packet switching. Another viable option is to use a large number of client signal ports in a muxponder configuration. FlexEthernet, which will be discussed in the next section, is advantageous to realize flexible client signals for the full benefit of optical agility applications. On the line side, an agile photonic architecture based on a flexible grid provides the ability to reroute optical signals, assign to them specific frequencies, and allocate bandwidths as needed across the network.

Multi-layer and multi-domain network management is another integral component. The software needs the ability to accomplish two important tasks. First, it needs to estimate the net system margin for capacity provisioning and path allocation. Second, it needs to perform re-optimization of the affected wavelengths when the network services change. These features can be naturally integrated into the emerging network architecture based on software-defined networks (SDNs) and network function virtualization (NFV). The result is the delivery of more agile and innovative services with lower CAPEX and OPEX [48]. A general architecture of SDN/NFV is depicted in Fig. 22. End-to-end orchestration and seamless integration across physical and virtual networks are enabled. The commercialization of SDN/NFV is in progress. For example, the SDN/NFV

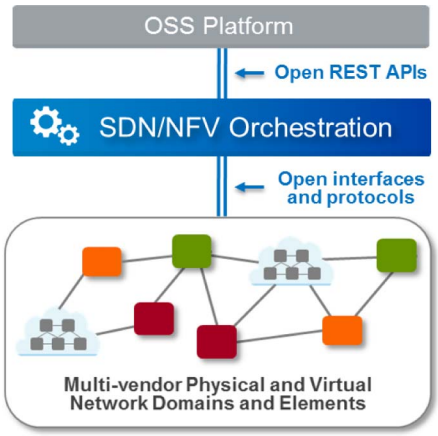

Fig. 22. Illustration of a SDN/NFV platform.

platform described in [49] uses a container-based microservices software architecture. This incorporates modeling, templating, and orchestration methodologies to provide a scalable, vendor-agnostic, and highly programmable software platform.

Optical network optimization comprises the adjustment of both the data rate of each transceiver and the optical launch power for each wavelength at each link node (transceiver, ROADM, and amplifier) [50,51]. The optical launch power determines the noise and intra-channel fiber nonlinearity to the channel itself and the inter-channel fiber nonlinearities to the other co-propagating channels. Convex channel power optimization has been proposed to maximize the minimum margin or aggregate communication rate [52].

VII. FlexEthernet and FlexOTN

To optimize network efficiencies and transport bandwidth utilization, especially for higher-capacity wavelengths or groups of wavelengths in a media channel, additional service layer flexibility is useful. Initiatives are underway in standards bodies to introduce flexible client interfaces on routers, switches, and optical transport equipment. FlexEthernet (FlexE) is specified in the OIF, with the first implementation agreement published in early 2016 [53]. FlexOTN, as specified in ITU-T/G.709.1, defines flexible OTN interfaces and was consented to in the fall of 2016.

Both FlexEthernet and FlexOTN dissociate clients/services from the physical gray interface/module (Fig. 23). FlexEthernet introduces a new shim layer between the existing IEEE-defined Ethernet PCS and MAC layers. It adds a new TDM frame structure using existing Ethernet building blocks, such as 66B and new ordered sets. FlexOTN utilizes existing OTN framing structures, group bonding, and LO ODU flex to achieve this flexible service/client layer.

FlexEthernet clients and FlexOTN clients provide granularities of $n \times 25$ Gb/s to match the desired line capacity. They provide methods of under-filing an interface without requiring flow control or other higher-layer schemes. An

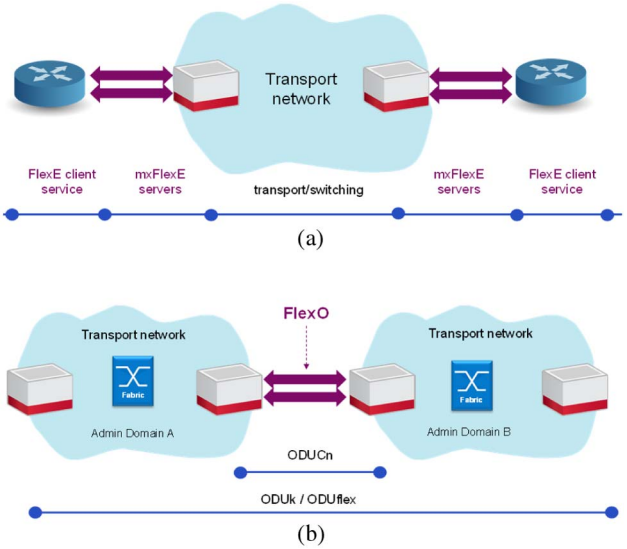

Fig. 23. (a) FlexEthernet and (b) FlexOTN architectures.

important benefit is that the service rate can be configured remotely to match a change in the transport line rate without any change to the physical connections.

VIII. Conclusion

Flexibility and agility should be exploited in future optical networks to satisfy the increased demand for traffic capacity. In this paper, we described building blocks and tools that will make these new networks a reality. Next-generation transceivers will enable bit rates from 100 to 600 Gb/s and, eventually, 1 Tb/s. They will operate at a higher baud rate and will require higher bandwidth components in InP and SiP technologies. Advances in DSP algorithms will further improve the performance of the next generation of flexible coherent transceivers. They will offer multi-dimensional modulation formats, constellation shaping, digital compensation of fiber nonlinearities, frequency-division multiplexing, and advances in FEC.

New software tools are being developed to achieve more efficient utilizations of networks, while at the same time providing network virtualization, orchestration, and simplification of management. Flexibility, from a service layer perspective, is incorporated into the FlexEthernet and FlexOTN standards to optimize network efficiencies and transport bandwidth utilization.

Acknowledgment

Portions of this work were presented at the Photonic Networks and Devices (NETWORKS) conference in 2016, “Beyond 100 Gb/s.”

References

[1] “Cisco visual networking index: Forecast and methodology, 2015–2020,” Cisco White Paper, 2016 [Online]. Available: http://www.cisco.com/c/en/us/solutions/collateral/service-provider/visual-networking-index-vni/complete-white-paper-c11-481360.pdf.

[2] K. Kikuchi, “Fundamentals of coherent optical fiber communications,” *J. Lightwave Technol.*, vol. 34, no. 1, pp. 157–179, 2016.

[3] C. Laperle and M. O’Sullivan, “Advances in high-speed DACs, ADCs, and DSP for optical coherent transceivers,” *J. Lightwave Technol.*, vol. 32, no. 4, pp. 629–643, 2014.

[4] K. Roberts, S. H. Foo, M. Moyer, M. Hubbard, A. Sinclair, J. Gaudette, and C. Laperle, “High capacity transport—100G and beyond,” *J. Lightwave Technol.*, vol. 33, no. 3, pp. 563–578, 2015.

[5] D. A. Morero, M. A. Castrillón, A. Aguirre, M. R. Hueda, and O. E. Agazzi, “Design tradeoffs and challenges in practical coherent optical transceiver implementations,” *J. Lightwave Technol.*, vol. 34, no. 1, pp. 121–136, 2016.

[6] F. R. Kschischang, “Forward error correction in roadmap of optical communications,” *J. Opt.*, vol. 18, pp. 23–24, 2016.

[7] K. Roberts and C. Laperle, “Flexible transceivers,” in *European Conf. on Optical Communication (ECOC)*, 2012, paper We.3.A.3.

[8] N. Sambo, P. Castoldi, A. D. Errico, E. Riccardi, A. Pagano, M. S. Moreolo, J. M. Fàbrega, D. Rafique, A. Napoli, S. Frigerio, E. H. Salas, G. Zervas, M. Nölle, J. K. Fischer, A. Lord, and J. P. F.-P. Gimenez, “Next generation sliceable bandwidth variable transponders,” *IEEE Commun. Mag.*, vol. 53, no. 2, pp. 163–171, 2015.

[9] H. Sun, K.-T. Wu, and K. Roberts, “Real-time measurements of a 40 Gb/s coherent system,” *Opt. Express*, vol. 16, no. 2, pp. 873–879, 2008.

[10] S. J. Savory, “Digital coherent optical receivers: Algorithms and subsystems,” *IEEE J. Sel. Top. Quantum Electron.*, vol. 16, no. 5, pp. 1164–1179, 2010.

[11] Q. Zhuge, M. Morsy-Osman, X. Xu, M. Chagnon, M. Qiu, and D. V. Plant, “Spectral efficiency-adaptive optical transmission using time domain hybrid QAM for agile optical networks,” *J. Lightwave Technol.*, vol. 31, no. 15, pp. 2621–2628, 2013.

[12] X. Zhou, L. E. Nelson, and P. Magill, “Rate-adaptable optics for next generation long-haul transport networks,” *IEEE Commun. Mag.*, vol. 51, no. 3, pp. 41–49, 2013.

[13] Q. Zhuge, M. Morsy-Osman, M. Chagnon, X. Xu, M. Qiu, and D. V. Plant, “Terabit bandwidth-adaptive transmission using low-complexity format-transparent digital signal processing,” *Opt. Express*, vol. 22, no. 3, pp. 2278–2288, 2014.

[14] “Spectral grids for WDM applications: DWDM frequency grid,” ITU-T Recommendation G.694.1, Feb. 2012 [Online]. Available: https://www.itu.int/rec/T-REC-G.694.1-201202-I/en.

[15] M. Y. S. Sowailem, T. M. Hoang, M. Morsy-Osman, M. Chagnon, D. Patel, S. Paquet, C. Paquet, I. Woods, O. Liboiron-Ladouceur, and D. V. Plant, “400-G single carrier 500-km transmission with an InP dual polarization IQ modulator,” *IEEE Photonics Technol. Lett.*, vol. 28, no. 11, pp. 1213–1216, 2016.

[16] Z. Zhang, C. Li, J. Chen, T. Ding, Y. Wang, H. Xiang, Z. Xiao, L. Li, M. Si, and X. Cui, “Coherent transceiver operating at 61-Gbaud/s,” *Opt. Express*, vol. 23, no. 15, pp. 18988–18995, 2015.

[17] H. Zhang, C. R. Davidson, H. G. Batshon, M. Mazurczyk, M. Bolshtyansky, D. G. Foursa, and A. Pilipetskii, “DP-16 QAM based coded modulation transmission in C+L band system at transoceanic distance,” in *Optical Fiber Communication Conf. (OFC)*, 2016, paper W1I.2.

[18] A. Ghazisaeidi, I. F. de Jauregui Ruiz, R. Rios-Muller, L. Schmalen, P. Tran, P. Brindel, A. C. Meseguer, Q. Hu, F. Buchali, G. Charlet, and J. Renaudier, "65Tb/s transoceanic transmission using probabilistically-shaped PDM-64QAM," in *European Conf. on Optical Communication (ECOC)*, 2016, paper Th.3.C.4.

[19] M. Filer, J. Gaudette, M. Ghobadi, R. Mahajan, T. Issenhuth, B. Klinkers, and J. Cox, "Elastic optical networking in the Microsoft cloud," *J. Opt. Commun. Netw.*, vol. 8, no. 7, pp. A45–A54, 2016.

[20] K. Schuh, F. Buchali, W. Idler, Q. Hu, W. Templ, A. Bielik, L. Altenhain, H. Langenhagen, J. Rupeter, U. Dümler, T. Ellermeyer, R. Schmid, and M. Möller, "100 GSa/s BiCMOS DAC supporting 400 Gb/s dual channel transmission," in *European Conf. on Optical Communication (ECOC)*, 2016, paper M.1.C.4.

[21] L. Kull, T. Toifl, M. Schmatz, P. A. Francese, C. Menolfi, M. Braendli, M. Kossel, T. Morf, T. Meyer Anderson, and Y. Leblebici, "A 90GS/s 8b 667mW 64× interleaved SAR ADC in 32nm digital SOI CMOS," in *Int. Solid-State Circuits Conf. (ISSCC)*, 2014, pp. 378–379.

[22] Y. Ogiso, T. Yamada, J. Ozaki, Y. Ueda, N. Kashio, N. Kikuchi, E. Yamada, H. Mawatari, H. Tanobe, S. Kanazawa, H. Yamazaki, Y. Ohiso, T. Fujii, M. Ishikawa, and M. Kohtoku, "Ultra-high bandwidth InP IQ modulator with 1.5 V Vπ," in *European Conf. on Optical Communication (ECOC)*, 2016, paper Tu.3.A.2.

[23] D. Patel, S. Ghosh, M. Chagnon, A. Samani, V. Veerasubramanian, M. Osman, and D. V. Plant, "Design, analysis, and transmission system performance of a 41 GHz silicon photonic modulator," *Opt. Express*, vol. 23, no. 11, pp. 14263–14287, June 2015.

[24] M. Morsy-Osman, M. Chagnon, X. Xu, Q. Zhuge, M. Poulin, Y. Painchaud, M. Pelletier, C. Paquet, and D. V. Plant, "Colorless and preamplifierless reception using an integrated Si-photonic coherent receiver," *IEEE Photonics Technol. Lett.*, vol. 25, no. 11, pp. 1027–1030, 2013.

[25] E. Agrell and M. Karlsson, "Power-efficient modulation formats in coherent transmission systems," *J. Lightwave Technol.*, vol. 27, no. 22, pp. 5115–5126, 2009.

[26] D. S. Millar, T. Koike-Akino, S. Ö. Arık, K. Kojima, K. Parsons, T. Yoshida, and T. Sugihara, "High-dimensional modulation for coherent optical communications systems," *Opt. Express*, vol. 22, no. 7, pp. 8798–8812, 2014.

[27] M. Reimer, S. O. Gharan, A. D. Shiner, and M. O'Sullivan, "Optimized 4 and 8 dimensional modulation formats for variable capacity in optical networks," in *Optical Fiber Communications Conf. and Exhibition (OFC)*, 2016, paper M3A.4.

[28] A. D. Shiner, M. Reimer, A. Borowiec, S. O. Gharan, J. Gaudette, P. Mehta, D. Charlton, K. Roberts, and M. O'Sullivan, "Demonstration of an 8-dimensional modulation format with reduced inter-channel nonlinearities in a polarization multiplexed coherent system," *Opt. Express*, vol. 22, no. 17, pp. 20366–20374, 2014.

[29] R. F. H. Fischer, *Precoding and Signal Shaping for Digital Transmission*. Wiley-IEEE, 2002.

[30] S. Zhang, F. Yaman, Y. K. Huang, J. D. Downie, D. Zou, W. A. Wood, A. Zakharian, R. Khrapko, S. Mishra, V. Nazarov, J. Hurley, I. B. Djordjevic, E. Mateo, and Y. Inada, "Capacity-approaching transmission over 6375 km at spectral efficiency of 8.3 bit/s/Hz," in *Optical Fiber Communications Conf. and Exhibition (OFC)*, 2016, paper Th5C.2.

[31] T. Fehenberger, A. Alvarado, G. Böcherer, and N. Hanik, "On probabilistic shaping of quadrature amplitude modulation for the nonlinear fiber channel," *J. Lightwave Technol.*, vol. 34, no. 21, pp. 5063–5073, 2016.

[32] K. Roberts, C. Li, L. Strawczynski, M. O'Sullivan, and I. Hardcastle, "Electronic pre-compensation of optical nonlinearity," *IEEE Photonics Technol. Lett.*, vol. 18, no. 2, pp. 403–405, 2006.

[33] E. Ip and J. M. Kahn, "Compensation of dispersion and nonlinear impairments using digital backpropagation," *J. Lightwave Technol.*, vol. 26, no. 20, pp. 3416–3425, 2008.

[34] Z. Tao, L. Dou, W. Yan, L. Li, T. Hoshida, and J. C. Rasmussen, "Multiplier-free intrachannel nonlinearity compensating algorithm operating at symbol rate," *J. Lightwave Technol.*, vol. 29, no. 17, pp. 2570–2576, Sept. 2011.

[35] F. Zhang, Q. Zhuge, M. Qiu, W. Wang, M. Chagnon, and D. V. Plant, "XPM model-based digital backpropagation for subcarrier-multiplexing systems," *J. Lightwave Technol.*, vol. 33, no. 24, pp. 5140–5150, 2015.

[36] Z. Tao, L. Dou, W. Yan, Y. Fan, L. Li, S. Oda, Y. Akiyama, H. Nakashima, T. Hoshida, and J. C. Rasmussen, "Complexity-reduced digital nonlinear compensation for coherent optical system," *Proc. SPIE*, vol. 8647, 86470K, 2013.

[37] Q. Zhuge, M. Reimer, A. Borowiec, M. O'Sullivan, and D. V. Plant, "Aggressive quantization on perturbation coefficients for nonlinear pre-distortion," in *Optical Fiber Communications Conf. and Exhibition (OFC)*, 2014, paper Th4D.7.

[38] S. Chandrasekhar, X. Liu, B. Zhu, and D. W. Peckham, "Transmission of a 1.2-Tb/s 24-carrier no-guard-interval coherent OFDM superchannel over 7200-km of ultra-large-area fiber," in *European Conf. on Optical Communication (ECOC)*, 2009, paper PD2.6.

[39] R. Dar and P. J. Winzer, "On the limits of digital back-propagation in fully loaded WDM systems," *IEEE Photonics Technol. Lett.*, vol. 28, no. 11, pp. 1253–1256, 2016.

[40] L. B. Du and A. J. Lowery, "Optimizing the subcarrier granularity of coherent optical communications systems," *Opt. Express*, vol. 19, no. 9, pp. 8079–8084, 2011.

[41] M. Qiu, Q. Zhuge, M. Chagnon, Y. Gao, X. Xu, M. Morsy-Osman, and D. V. Plant, "Digital subcarrier multiplexing for fiber nonlinearity mitigation in coherent optical communication systems," *Opt. Express*, vol. 22, no. 15, pp. 18770–18777, 2014.

[42] P. Poggiolini, A. Nespola, Y. Jiang, G. Bosco, A. Carena, L. Bertignono, S. M. Bilal, S. Abrate, and F. Forghieri, "Analytical and experimental results on system maximum reach increase through symbol rate optimization," *J. Lightwave Technol.*, vol. 34, no. 8, pp. 1872–1885, 2016.

[43] J. X. Cai, M. Mazurczyk, O. V. Sinkin, M. Bolshtyansky, D. G. Foursa, and A. Pilipetskii, "Experimental study of subcarrier multiplexing benefit in 74 nm bandwidth transmission up to 20,450 km," in *European Conf. on Optical Communication (ECOC)*, 2016, pp. 1–3.

[44] S. Lin and D. J. Costello, Jr., *Error Control Coding*, 2nd Ed., Upper Saddle River, NJ: Pearson Prentice Hall, 2004.

[45] M. Jinno, T. Ohara, Y. Sone, A. Hirano, O. Ishida, and M. Tomizawa, "Elastic and adaptive optical networks: Possible adoption scenarios and future standardization aspects," *IEEE Commun. Mag.*, vol. 49, no. 10, pp. 164–172, 2011.

[46] O. Gerstel, M. Jinno, A. Lord, and S. J. B. Yoo, "Elastic optical networking: A new dawn for the optical layer?" *IEEE Commun. Mag.*, vol. 50, no. 2, pp. s12–s20, 2012.

[47] "Transforming margin into capacity with liquid spectrum," Ciena White Paper, 2016 [Online]. Available: http://media.ciena.com/documents/Transforming_Margin_into_Capacity_with_Liquid_Spectrum_WP.pdf.

[48] "NFV and SDN: The next step in the evolution of the networks," Ciena White Paper, 2016 [Online]. Available: http://media.ciena.com/documents/+NFV+and+SDN+The+Next+Step+in+the+Evolution+of+the+Networks+ENG.pdf.

[49] "Blue planet SDN and NFV are changing the game," Ciena White Paper, 2016 [Online]. Available: http://media.ciena.com/documents/SDN-NFV-Are-Changing-The-Game-WP.pdf.

[50] D. J. Ives, P. Bayvel, and S. J. Savory, "Adapting transmitter power and modulation format to improve optical network performance utilizing the Gaussian noise model of nonlinear impairments," *J. Lightwave Technol.*, vol. 32, no. 21, pp. 4087–4096, 2014.

[51] L. Yan, E. Agrell, H. Wymeersch, and M. Brandt-Pearce, "Resource allocation for flexible-grid optical networks with nonlinear channel model [Invited]," *J. Opt. Commun. Netw.*, vol. 7, no. 11, pp. B101–B108, 2015.

[52] I. Roberts, J. M. Kahn, and D. Boertjes, "Convex channel power optimization in nonlinear WDM systems using Gaussian noise model," *J. Lightwave Technol.*, vol. 34, no. 13, pp. 3212–3222, 2016.

[53] OIF, "Flex Ethernet implementation agreement," IA #OIF-FLEXE-01.0, Mar. 2016 [Online]. Available: http://www.oiforum.com/wp-content/uploads/OIF-FLEXE-01.0.pdf.

132.206.69.32 {ts '2017-02-03 22:44:28'}